Progress in Nuclear Energy 52 (2010) 555–562

Contents lists available at ScienceDirect

Progress in Nuclear Energy

journal homepage: www.elsevier.com/locate/pnucene

# Flow regime identification and volume fraction prediction in multiphase flows by means of gamma-ray attenuation and artificial neural networks

César Marques Salgado [a], Cláudio M.N.A. Pereira [a,*], Roberto Schirru [b], Luis E.B. Brandão [a]

[a] Instituto de Engenharia Nuclear, DIRA/IEN/CNEN, Rio de Janeiro, CEP: 21945-970, Caixa Postal 68550, Brazil
[b] Universidade Federal do Rio de Janeiro, [PEN/COPPE-DNC/EE]CT, Rio de Janeiro, CEP: 21941-972, Caixa Postal 68509, Brazil

*Keywords:*
NaI detector
Monte Carlo simulation
Volume fraction
Artificial neural network
Gamma-ray

A B S T R A C T

This work presents a new methodology for flow regimes identification and volume fraction predictions in water–gas–oil multiphase systems. The approach is based on gamma-ray pulse height distributions (PHDs) pattern recognition by means the artificial neural networks (ANNs). The detection system uses appropriate fan beam geometry, comprised of a dual-energy gamma-ray source and two NaI(Tl) detectors adequately positioned in order measure transmitted and scattered beams, which makes it less dependent on the regime flow. The PHDs are directly used by the ANNs without any parameterization of the measured signal. The system comprises four ANNs. The first identifies the flow regime and the other three ANNs are specialized in volume fraction predictions for each specific regime. The ideal and static theoretical models for annular, stratified and homogeneous regimes have been developed using MCNP-X mathematical code, which was used to provide training, test and validation data for the ANNs. The energy resolution of NaI(Tl) detectors is also considered on the mathematical model. The proposed ANNs could correctly identify all three different regimes with satisfactory prediction of the volume fraction in water–gas–oil multiphase system, demonstrating to be a promising approach for this purpose.


## 1. Introduction

Multiphase flow measurement is a very important issue in offshore petroleum industries. The use of techniques for determination volume fractions of oil–water–gas flows with adequate precision is required. Commonly, such techniques are invasive, and involves in high cost associated to installation and maintenance. On the other hand, non-invasive techniques tend to be less accurate. Due to this fact, many investigations on non-invasive techniques are found in literature with the aim of improving accuracy and reducing costs.

By using gamma-ray sources (Abouelwafa and Kendall, 1980; Johansen et al., 1994; Åbro et al., 1998,1999; Tjugum et al., 2001, 2002) it is possible to perform these measurements without modifying the operational conditions, allowing accomplishment of the entire monitoring process. However, volume fraction prediction by using gamma-ray measurements generally depends on the correct identification of the flow regime to increase the precision in prediction. The flow regime information in the liquid-gas flows is usually obtained by individual interpretation and subjective evaluations based on visual observations (graphic illustrations). The major difficulty in visual observation, even when using high-speed photography, is that the picture is often confusing and difficult to interpret, especially when dealing with high velocity flows. In addition, there are systems that are opaque where flow visualization is impossible; then, such analysis is also not possible by this method (Haojiang et al., 2001; Jin et al., 2003). Therefore, a non-invasive system that can provide material volume fraction (MVF) predictions regardless of a priori knowledge of the flow regime, without subjective evaluation, is a great contribution.

Together with the detection system, artificial neural networks (ANNs) (Haykin, 1999) has been used in order to interpret the pulse height distributions (PHDs) obtained by gamma-ray radiation detectors to identify the flow regime (Mi et al., 1997, 1998, Haojiang et al., 2001; Jin et al., 2003) and predict the MVFs (Salgado et al., 2007, 2009, Bishop and James, 1992; Åbro et al., 1999). ANNs are mathematical models inspired in the human brain, which has the ability of learning by examples. ANNs are able to discover behaviors and patterns from a finite set of data (called the “training set” or “training patterns”). If an adequate training set is provided, the ANN is able to generalize the knowledge acquired during (learning) process, responding adequately to new situations (not comprised in the training set).

* Corresponding author. Tel.: +55 21 2173 3897; fax: +55 21 2173 3852.
*E-mail address:* cmnap@ien.gov.br (C.M.N.A. Pereira).

0149-1970/$ – see front matter © 2010 Elsevier Ltd. All rights reserved.
doi:10.1016/j.pnucene.2010.02.001

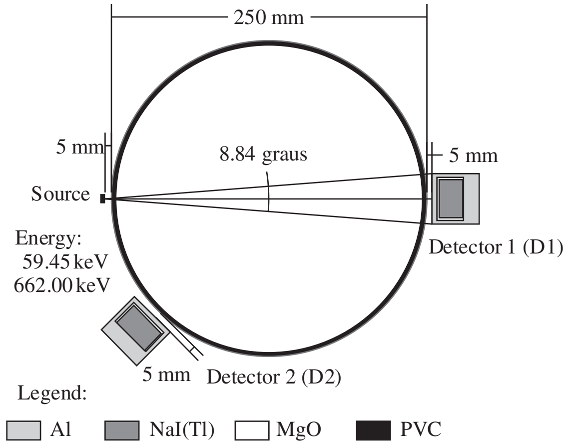


**Fig. 1.** Simulated system.

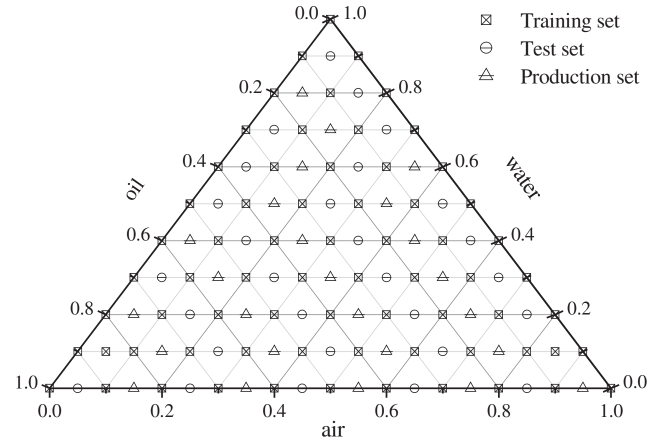


**Fig. 3.** Training, test and production sets.

The training and test patterns (different volume fractions for the three flow regimes) were obtained by means of static and ideal mathematical models for annular, stratified and homogeneous regimes.

These models were developed by mathematical simulation using the Monte Carlo N-Particle eXtended (X-5 Monte Carlo Team, 2003) (MCNP-X) computer code (Pelowitz, 2005) based on the method of Monte Carlo (MC) (Åbro et al., 1998,1999). The MC technique is a widely used simulation tool for radiation transport, mainly in situations where physical measurements are inconvenient or impracticable. In this work the MCNP-X code, which is specific for simulating electron and photon transport through materials with various geometries, has been used. The model developed in the MCNP-X code considers the main effects of radiation with the matter involved and the PHDs from the NaI(Tl) detectors. The energy resolution, dimensions and characteristics of a real detector are also considered; in general, the model presented tends to approach the realistic case.

In this work, the whole gamma-ray PHDs obtained by detectors are directly used to feed the ANNs without any parameterization of the signal, which allowed the use of simplified detection geometry consists of two NaI(Tl) detectors, the first one positioned at 180° diametrically opposed to sources of $^{241}$Am and $^{137}$Cs and the second one at 45°. In addition, the system considers the transmitted ($I_T$) and scattered ($I_S$) beam measurements in order to increase the visualization of the cross-section, making the response less dependent on the flow regime and also to obtain sufficient information to determine precisely the volume fractions regardless, a priori, of the flow regime.

The developed ANN system comprises four ANNs. The first one is trained to identify the dominant flow regime and other ones are trained for volume fraction predictions of each specifically regime. An evaluation of the quality training of ANN was made from 25 patterns not used during the training phase, also generated by mathematical code.

In this study, the training patterns (combination of the volume fractions of each material) were uniformly distributed throughout the search space; moreover, the choice of each data set was performed systematically. Another important enhancement over the mathematical model used in previous work (Salgado et al., 2009) is the use of a more realistic model of the NaI(Tl) detector, considering the real dimensions and materials compositions, as well as its energy resolution. These improvements allowed the achievement of the better results, showing smaller average relative errors for annular, stratified and homogeneous regimes with the use of only two detectors.

Thus, this work provides a new methodology, able to identify the flow regime with good accuracy and calculate volume fractions of multiphase flows (gas–water–oil) based on interpretation of gamma-ray PHDs by means of the ANNs, independently of a priori knowledge of the flow regime.

## 2. Proposed methodology

### *2.1. Volume fraction predictions*

#### *2.1.1. Mathematical detector model*

The mathematical model considered NaI(Tl) scintillator detector as a homogeneous cylinder (Salgado et al., 2008; Berger and Seltzer,

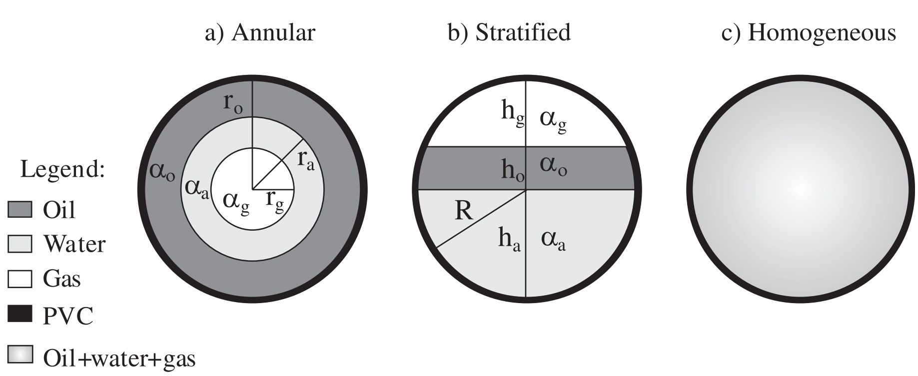


**Fig. 2.** The models for the different annular, stratified and homogeneous flow regimes.

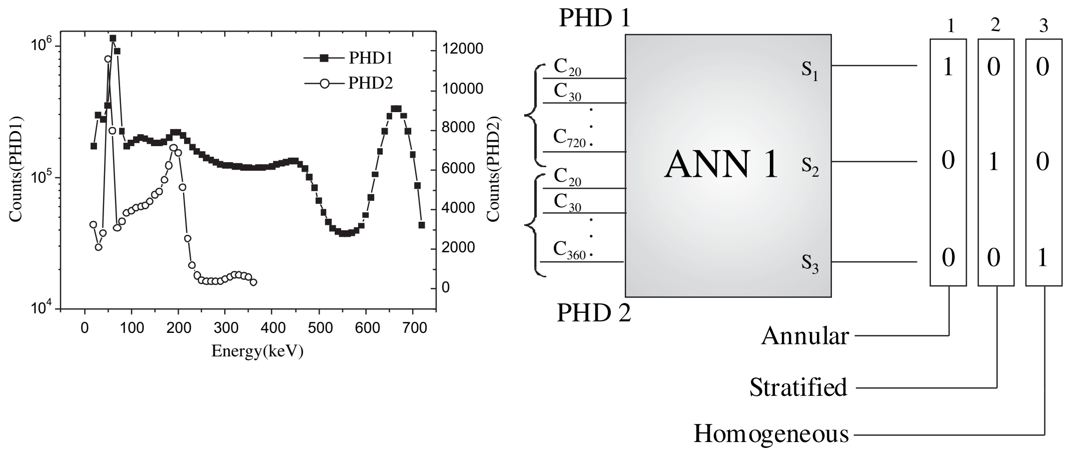


**Fig. 4.** Schematic representation used for the ANN.

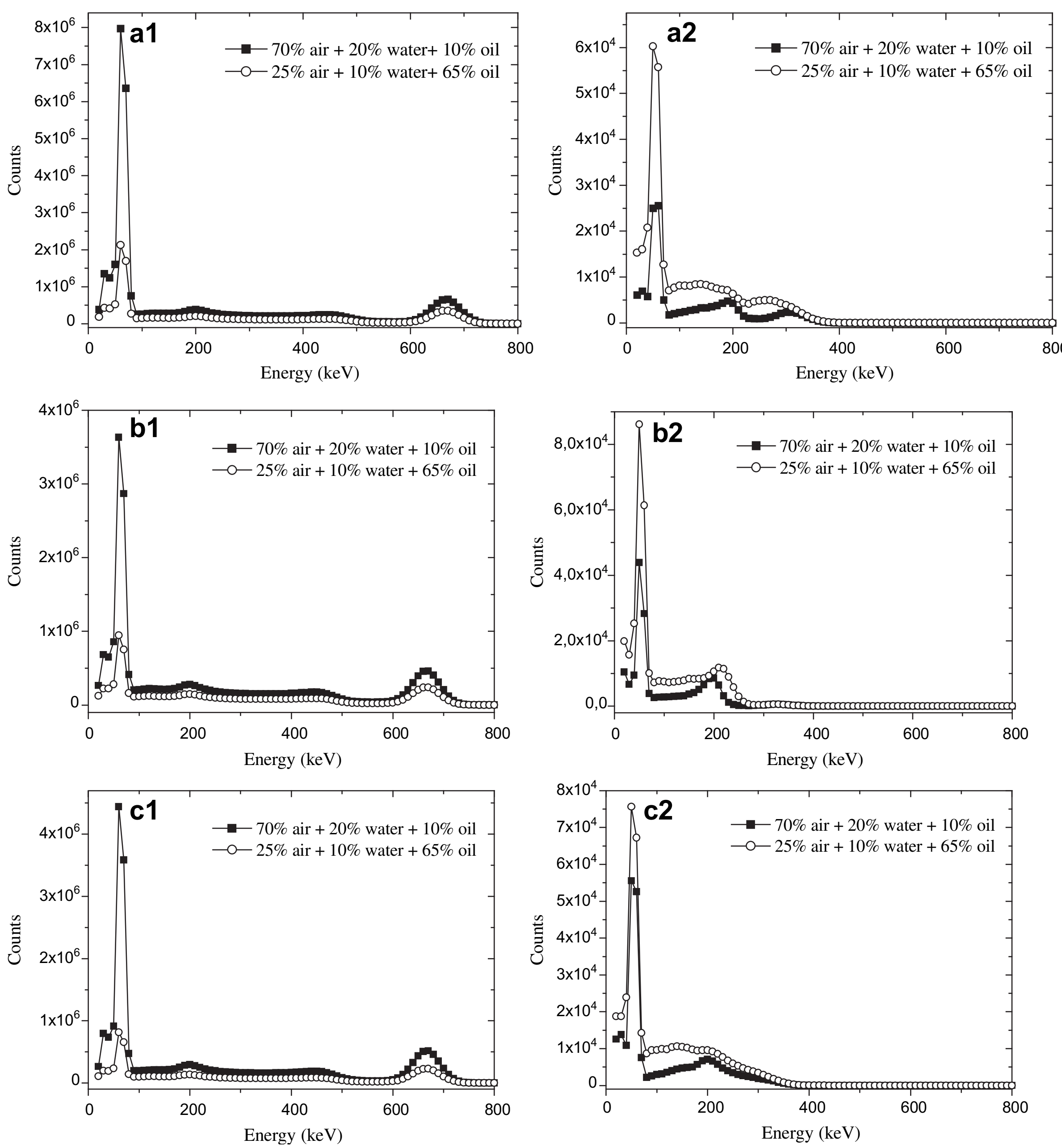


**Fig. 5.** PHD generated by MCNP-X code for regimes: annular: a1) D1 e a2) D2; stratified: b1) D1 e b2) D2; homogeneous: c1) D1 e c2) D2.

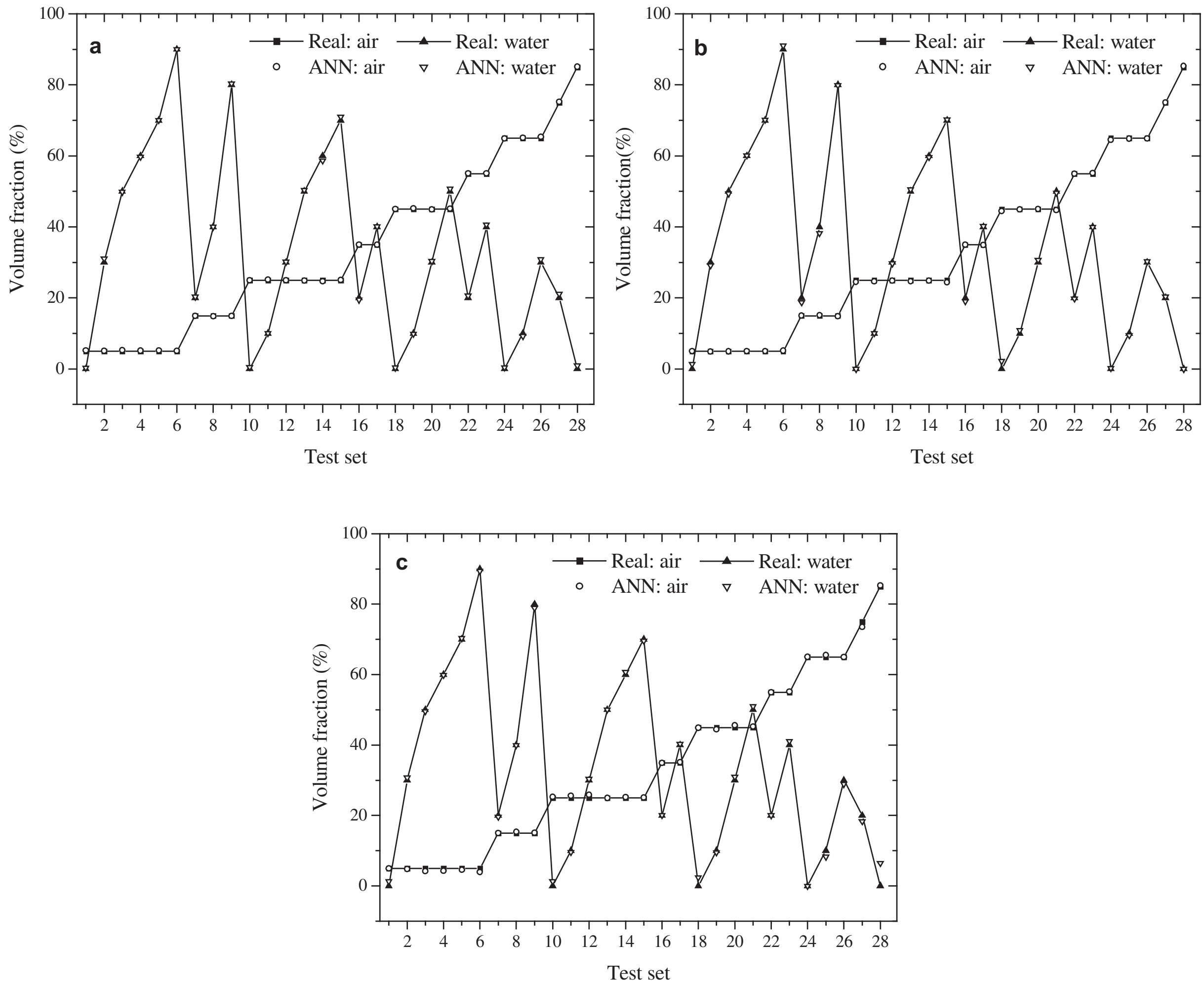


**Fig. 6.** Results obtained for the test set on regime: a) Annular; b) Stratified; c) Homogeneous.

1972; Saito and Moriuchi, 1981; Orion and Wilopolski, 2002; Shi et al., 2002; Sood and Gardner, 2004) with 31 mm (diameter) × 19 mm (thickness). The information (dimensions and materials) of a real NaI(Tl) detector was considered in the mathematical model for calculating the MCNP-X code from gammagraphy[1] technique. A special treatment provided in the MCNP-X code: the Gaussian energy broadening[2] (GEB) (card FTn) option has been used to better fit the full energy peak shape of PHD (Pelowitz, 2005). The GEB parameters have been set taking into account[3] the resolution of the detector by means of the FWHM provided by radioactive sources (Salgado et al., 2008), for this it must to be inserted into the input file (INP), the mathematical model of the detector. In calculations it has been considered the radiation background and the contributions due to interactions by Compton Effect.

### 2.1.2. *Proposed geometry*

The proposed geometry combines transmission ($I_T$) (at detector 1) and scattered ($I_s$) (at detector 2) radiation (dual-mode densitometry) from gamma-ray source with a fan beam, thus it is possible to acquire sufficient information about the flow regime and also to increase the measurement area on the cross-section of the pipe making the MVF prediction less dependent on the flow regime (Johansen and Jackson, 2000; Tjugum et al., 2001).

In all simulations, fan beam geometry (for the source) and two NaI(Tl) detectors has been used. One of them (D1) is aligned to the source (180°) and the other (D2) is located at 45°. The measurement system simulation is shown in Fig. 1. One collimated (angle beam 8.84°) gamma-ray point source (59.45 keV: $^{241}$Am and 662 keV: $^{137}$Cs) has also been simulated in the MCNP-X code. In our studies, salt water was used (4% of NaCl) to simulate the seawater (Johansen and Jackson, 2000).

The gaseous phase was substituted by air and oil was assumed as a hydrocarbon (molecular formula $C_5H_{10}$) with a 0.896 g cm$^{-3}$ density (Hussein and Han, 1995). A Polyvinyl Chloride (PVC) tube

**Table 1**
Summary of pattern recognition for the prediction results.

| Detectors | Annular | | Stratified | | Homogeneous | |
|---|---|---|---|---|---|---|
| D1 e D2 | Air | Water | Air | Water | Air | Water |
| ≤ 5% | 90.083 | 76.033 | 90.909 | 72.727 | 85.950 | 70.248 |
| 5–10% | 0.826 | 4.959 | 0 | 9.091 | 1.653 | 9.091 |
| 10–20% | 0 | 1.653 | 0 | 0.826 | 2.479 | 2.479 |
| 20–30% | 0 | 0 | 0 | 0 | 0.826 | 0.826 |
| > 30% | 0 | 0 | 0 | 0 | 0 | 0 |
| $r^2$ | 1.0000 | 0.9998 | 1.0000 | 0.9996 | 0.9999 | 0.9992 |

[1] Gammagraphy is a non-destructive testing method consisting in carrying out a radiograph by using the electromagnetic gamma radiation of a radionuclide.

[2] The energy peaks behave like a Gaussian function.

[3] This step aims to validate the response of the detector quality by means of energy resolution while the order quantity will be achieved by normalize the of the full energy peak from PHD obtained by MCNP-X.

**Table 2**
ANN prediction for the production set on annular, stratified and homogeneous regimes.

| Pattern | Annular | | | | Stratified | | | | Homogeneous | | | |
|---|---|---|---|---|---|---|---|---|---|---|---|---|
| | Air (%) | | Water (%) | | Air (%) | | Water (%) | | Air (%) | | Water (%) | |
| | Real | RNA | Real | RNA | Real | RNA | Real | RNA | Real | RNA | Real | RNA |
| 1 | 5 | 5.00 | 20 | 19.58 | 5 | 4.97 | 20 | 18.85 | 5 | 5.04 | 20 | 20.67 |
| 2 | 5 | 5.24 | 40 | 40.67 | 5 | 4.97 | 40 | 40.02 | 5 | 5.12 | 40 | 41.07 |
| 3 | 5 | 5.12 | 80 | 79.69 | 5 | 5.08 | 80 | 80.50 | 5 | 4.44 | 80 | 80.14 |
| 4 | 15 | 15.02 | 0 | 0.51 | 15 | 14.90 | 0 | 0.00 | 15 | 15.21 | 0 | 0.00 |
| 5 | 15 | 15.03 | 10 | 9.80 | 15 | 15.02 | 10 | 9.31 | 15 | 15.19 | 10 | 10.05 |
| 6 | 15 | 14.98 | 30 | 29.37 | 15 | 15.08 | 30 | 28.82 | 15 | 15.70 | 30 | 30.03 |
| 7 | 15 | 14.79 | 50 | 49.44 | 15 | 15.08 | 50 | 49.50 | 15 | 14.56 | 50 | 49.72 |
| 8 | 15 | 14.86 | 60 | 59.41 | 15 | 15.16 | 60 | 60.26 | 15 | 14.86 | 60 | 59.38 |
| 9 | 15 | 14.76 | 70 | 68.83 | 15 | 15.23 | 70 | 68.50 | 15 | 14.58 | 70 | 69.80 |
| 10 | 25 | 25.17 | 20 | 19.10 | 25 | 24.82 | 20 | 19.14 | 25 | 25.70 | 20 | 21.28 |
| 11 | 25 | 24.76 | 40 | 39.93 | 25 | 24.64 | 40 | 41.09 | 25 | 24.69 | 40 | 38.98 |
| 12 | 35 | 34.83 | 0 | 0.07 | 35 | 34.35 | 0 | 0.45 | 35 | 34.68 | 0 | 0.76 |
| 13 | 35 | 34.98 | 10 | 9.95 | 35 | 34.75 | 10 | 9.83 | 35 | 34.81 | 10 | 10.28 |
| 14 | 35 | 34.52 | 30 | 29.82 | 35 | 35.01 | 30 | 30.39 | 35 | 34.88 | 30 | 29.97 |
| 15 | 35 | 34.95 | 50 | 49.01 | 35 | 35.03 | 50 | 50.11 | 35 | 35.23 | 50 | 49.63 |
| 16 | 35 | 34.92 | 60 | 61.06 | 35 | 34.77 | 60 | 60.26 | 35 | 34.64 | 60 | 59.36 |
| 17 | 45 | 44.78 | 20 | 19.92 | 45 | 45.08 | 20 | 20.38 | 45 | 45.16 | 20 | 19.57 |
| 18 | 45 | 44.80 | 40 | 39.74 | 45 | 45.05 | 40 | 39.46 | 45 | 45.21 | 40 | 39.06 |
| 19 | 55 | 55.15 | 0 | 0.65 | 55 | 54.55 | 0 | 2.14 | 55 | 54.72 | 0 | 1.53 |
| 20 | 55 | 54.75 | 10 | 9.35 | 55 | 55.10 | 10 | 10.71 | 55 | 54.95 | 10 | 8.09 |
| 21 | 55 | 54.93 | 30 | 30.31 | 55 | 55.00 | 30 | 30.10 | 55 | 55.81 | 30 | 28.25 |
| 22 | 65 | 64.97 | 20 | 20.58 | 65 | 64.68 | 20 | 18.93 | 65 | 65.55 | 20 | 18.33 |
| 23 | 75 | 75.04 | 0 | 0.00 | 75 | 75.15 | 0 | 0.17 | 75 | 75.21 | 0 | 4.59 |
| 24 | 75 | 74.94 | 10 | 9.79 | 75 | 75.11 | 10 | 9.01 | 75 | 73.15 | 10 | 8.43 |
| 25 | 95 | 95.63 | 0 | 0.67 | 95 | 94.78 | 0 | 3.84 | 95 | 95.75 | 0 | 0.00 |

composes a test section with 1.8 cm thickness and 25.0 cm of internal diameter. The models for the different flow regimes are shown in Fig. 2.

### 2.1.3. ANN training data

The first step in this investigation was the mathematical simulations for the different flow regimes (annular, stratified and homogeneous regimes), shown in Fig. 2, by means of MCNP-X code, in order to generate the training and test data sets for the ANNs. The values of the thickness (rg, rw and ro – annular model, see Fig. 2(a) and hg, hw e ho – stratified model see Fig. 2(b)), of each material had been varied, in the MCNP-X code, in order to generate a diverse combinations of MVF– $\alpha$w, $\alpha$g e $\alpha$o, while for the homogeneous regime mass fraction of each one of the materials had been varied. For each one of these combinations, which had been varied from 0% to 100%, the relative counts from transmitted ($I_T$) and scattered ($I_S$) beams had been calculated. It is important to emphasize that the MCNP-X code considers the material in a region (cell), defined in the INP, as uniform.

Volume fractions that compose training, test and production data sets are shown in Fig. 3, which presents a graphical representation called ternary.

Thus, a set of 363 (121 $\times$ 3) simulations for different combinations of MVFs and three flow regimes (annular, stratified and homogeneous) were made, in order to generate the training set of the ANNs (204 (68 $\times$ 3) simulations), test (84 (28 $\times$ 3) simulations) and production (75 (25 $\times$ 3) simulations). The test set was used for stopping criteria: cross validation (Haykin, 1999) in order to avoid over-training. The production set is used for a final validation test after training of the ANN, simulating the operating phase.

In this work, a 3-layer feed-forward multilayer perceptron (MLP) (Haykin, 1999) has been used. The learning/training algorithm was the back-propagation algorithm (Chauvin and Rumelhart, 1995). The ANN inputs and outputs are given by:

(i) ANN inputs[4] (106 neurons):
PHD1: 20–720 keV, with steps of 10 keV ($C_{20}$, $C_{30}$, …, $C_{720}$ – counts from channel 2 to 72);
PHD2: 20–360 keV, with steps of 10 keV ($C_{20}$, $C_{30}$, …, $C_{350}$ – counts from channel 2 to 35).
(ii) ANN outputs (2 neurons):
$H_2O$ volume fraction
Air volume fraction.

Note that only two phases are used as ANN outputs. The third phase is obtained by complement. Such set of volume fractions used as ANN outputs has been empirically chosen, after investigating (by experimentation) all possible combinations (including the use of three volume fractions).

### 2.2. Identification of regimes for ANN

The methodology consists on use the gamma-ray PHDs to feed the ANN1 in order to automatically identify the flow regime of this system. A schematic representation used for the proposed ANN is shown in Fig. 4.

[4] The energy range choice of each PHD used in the training took into account the value of relative error (R) below 10% in the counts, percentage acceptable according to the MCNP-X manual.

**Table 3**
Results of the ANNs training.

| Flow regime | $r^2$ | | Relative[a] error (%) | |
|---|---|---|---|---|
| | All patterns | | Production set | |
| | Air | Water | Air | Water |
| Annular | 1.0000 | 0.9998 | 0.73 | 1.48 |
| Stratified | 1.0000 | 0.9996 | 0.61 | 2.56 |
| Homogeneous | 0.9998 | 0.9989 | 1.73 | 3.31 |

[a] The patterns with no presence of any material (e.g. 0% of air) were not considered in the calculation of relative error.

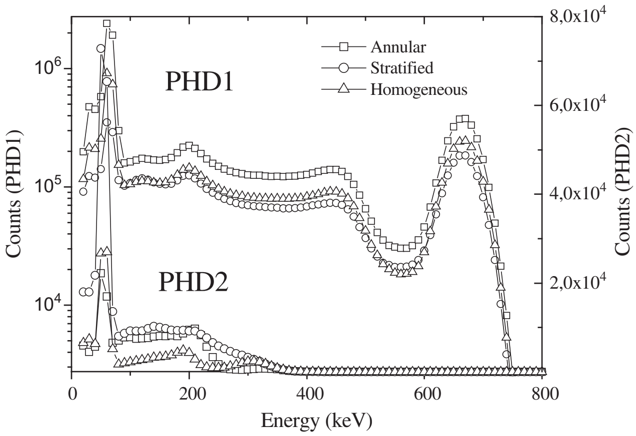


**Fig. 7.** PHDs obtained by MCNP-X code for different flow regimes.

The ANN used was a 3-layer feed-forward multilayer perceptron (MLP) (Haykin, 1999) trained by back-propagation algorithm It is important to note that patterns that contain only one material (e.g. 100% air) were removed of training set, since they represent the same flow regime, therefore, if considered they could confuse the of the ANN training. The ANN inputs and outputs are given by:

i) ANN inputs (106 neurons):
PHD1: 20–720 keV, with steps of 10 keV ($C_{20}$, $C_{30}$, –, $C_{720}$ – counts from channel 2 to 71);
PHD2: 20–360 keV, with steps of 10 keV ($C_{20}$, $C_{30}$, –, $C_{350}$ – counts from channel 2 to 35).

ii) ANN outputs (3 neurons)
$S_3$, $S_2$ and $S_1$

The output data were classified considering three neurons in ANN output ($S_3$, $S_2$ and $S_1$), so that to obtain the identification of systems, just that the ANN set the highest value among the network outputs to "1" corresponding to dominant flow regime and to "0" the others. To illustrate, suppose that the flow regime is annular, then the network should adjust the output for $S_3 = 0$, $S_2 = 0$ and $S_1 = 1$.

## 3. Methods application and results

### 3.1. Volume fraction determination

For illustration of the differences between the PHDs for each volume fraction some simulated transmitted ($I_T$) and scattered ($I_S$) beam measurements obtained by detector 1 and 2 respectively for the three flow regimes with two different volume fraction configurations are shown in Fig. 5. The PHD energy range considered here was 20–800 keV.

The prediction for the test set of the annular, stratified and homogeneous regimes are shown in Fig. 6 indicating that the ANNs could adequately predict volume fractions. Note excellent agreement between the volume fraction of the actual and predicted by ANNs showing the ability of generalization of the networks.

The ANNs performance of the MVF predictions is summarized in Table 1. As can be seen in Table 1, the ANNs could predict more than 70% of all patterns with errors less than 5% (worst case) for air, and about 80% less than 10% (worst case) for water volume fractions. The patterns with no air (0%) (9.09% of total) and of water (17.35% of

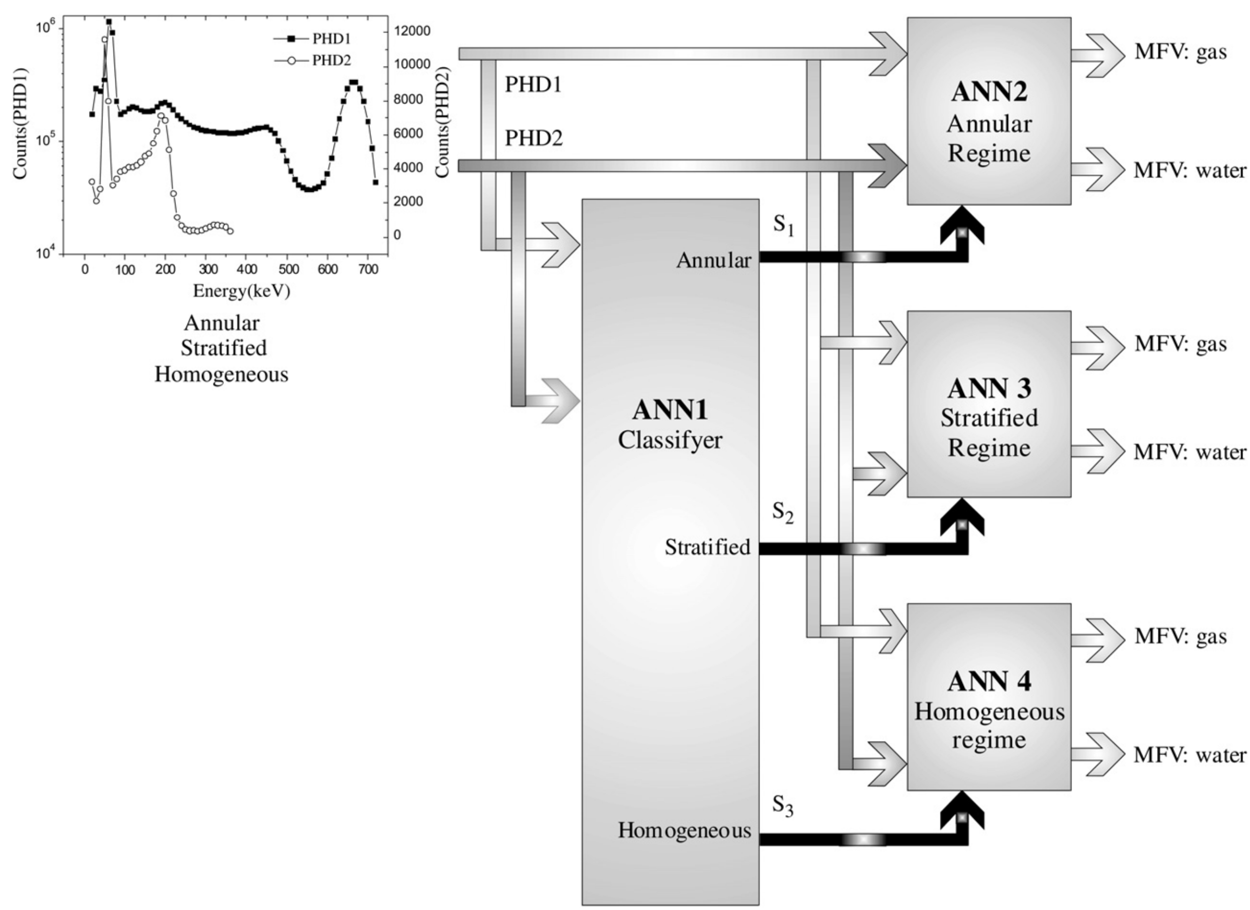


**Fig. 8.** Flow regime identification system and volume fraction predictions intelligent system.

total) not were considered, and then the ANNs classified 95% of all data for air and water volume fractions to within ±10% error for all regimes studied.

In Table 2, results obtained for the production set on annular, stratified and homogeneous regimes are presented. These results demonstrate a good generalization of the trained ANNs, indicating their ability for volume fraction predictions on annular, stratified and homogeneous regimes.

Linear models were fit to the data from the correlation between the volume fractions of the actual and predicted by the ANNs for all patterns and also for the production set using a least-squares procedure and linear correlation coefficients ($r^2$). The results are summarized in Table 3, demonstrating a good convergence of ANNs (ANN2, ANN3 and ANN4) about all data set in MVFs prediction for the three regimes studied.

### 3.2. Regime identification

To illustrate the difference between the flow regimes PHD some transmitted and scattered beam measurements of volume fraction of 30% air, 20% water and 50% oil for annular, stratified and homogeneous regimes are presented Fig. 7.

It is important emphasize that the networks (ANN2, ANN3 and ANN4) are suitably trained for the annular, stratified or homogeneous regimes, as described in item 3.1 and that the information used in the ANN1 training are the same PHDs (PHD 1 and PHD 2) used to calculate the volume fractions.

A simplified diagram of the proposed system for the identification of flow regimes with prediction of MVFs is shown in Fig. 8.

The proposed ANN reached 100% of accuracy, identifying all flow regimes submitted for a total of 354 patterns. The production set with 75 patterns was used in order to validate the ANN1 in working phase also presented 100% of correct classification.

## 4. Conclusions

In this work, several improvements related to methodologies for regime flows identification and volume fraction predictions were achieved.

A compact detection system, with two detectors, could be developed in order to provide adequate measurements for identifications and predictions. The use of non-parameterized PHD, probably contributed to this, providing more complete information about measured spectra.

The use of MCNP code was adequate to model the detection system and effects of radiation interaction with matter, allowing a very close to real representation. Hence, data for training the ANNs could be easily generate by MCNP simulation, avoiding the use of experimental data.

The ANNs architecture, as illustrated in Fig. 8, allows volume fractions to be predicted without knowledge about the flow regime. It has been possible due to the accuracy obtained for ANN1 (responsible to regime identification), which were able to correctly identify 100% of the actual regimes (among the possible ones).

Volume fraction predictions, by ANN2 (annular), ANN3 (stratified) and ANN4 (homogeneous), presented very good results, with maximum relative errors bellow 3.5%.

In summary, the proposed methodology demonstrated to contribute to the state-of-art in multiphase flow regime characterization, improving the following points: i) detection system is more compact; ii) the accuracy of ANN are improved; iii) the volume fractions can be automatically predicted without a priori knowledge of the actual flow regime.

The proposed methodology demonstrated to be quite promising. However, investigation on dynamic flows (in future work), in which proposed methodology should be adapted and improved, is required for real-world application. To accomplish that, an experimental facility is under development in the Institute.

## Acknowledgments

The authors would like to thank Ademir Xavier da Silva for allowing the use of the MCNP-X code of the Universidade Federal do Estado do Rio de Janeiro (UFRJ).

Claudio M. N. A. Pereira and Roberto Schirru are supported by Conselho Nacional de Desenvolvimento Científico e Tecnológico (CNPq) and Fundação de Amparo à Pesquisa do Estado do Rio de Janeiro (FAPERJ).

## References

Abouelwafa, M.S.A., Kendall, E.J.M., 1980. The measurement of component ratios in multiphase systems using gamma-ray attenuation. Journal of Physics E: Scientific Instruments 13, 341–345.
Åbro, E., Johansen, G.A., Opedal, H., 1998. A radiation transport model as a design tool for gamma densitometers. Nuclear Instruments and Methods in Physics Research A431, 347–355.
Åbro, E., Khoryakov, V.A., Johansen, G.A., Kocbach, L., 1999. Determination of void fraction and flow regime using a neural network trained on simulated data based on gamma-ray densitometry. Measurement Science and Technology 10, 619–630.
Berger, M.J., Seltzer, S.M., 1972. Response functions for sodium iodide scintillation detectors. Nuclear Instruments and Methods 104, 317–332.
Bishop, C.M., James, G.D., 1992. Analysis of multiphase flows using dual-energy gamma densitometry and neural networks. Nuclear Instruments and Methods A 327, 580.
Chauvin, Y., Rumelhart D.E., 1995. Backpropagation Theory, Architectures and Applications.
Haojiang, W., Fangde, Z., Yuyuan, W., 2001. Intelligent identification system of flow regime of oil–gas–water multiphase flow. International Journal of Multiphase Flow 27, 459–475.
Haykin, S., 1999. Neural Networks: A Comprehensive Foundation Prentice Hall 2nd edition.
Hussein, E.M.A., Han, P., 1995. Phase volume-fraction measurement in oil–water–gas flow using fast neutrons. Nuclear Geophysics 9 (3), 229–234.
Jin, N.D., Nie, X.B., Ren, Y.Y., Liu, X.B., 2003. Characterization of oil/water two-phase flow patterns based on nonlinear time series analysis. Flow Measurement and Instrumentation 14, 169–175.
Johansen, G.A., Jackson, P., 2000. Salinity independent measurement of gas volume fraction in oil/gas/water pipe flows. Applied Radiation and Isotopes 53, 595–601.
Johansen, G.A., Froystein, T., Hjertaker, B.T., Isaksen, Ø., Olsen, Ø., Strandos, S.K., Olsen, T.S., Åbro, E., Mckibben, B., Heggstad, S. and Hammer, E., 1994. The design of a dual mode tomography for three-component flow imaging. In: Proceedings of European Concerted Action of Process Tomography (ECAPT), Oporto, Portugal, March, pp. 24–27.
Mi, Y., Tsoukalas, L.H., Ishii, M., 1997. Application of multiple self-organizing neural networks: flow pattern classification. Transactions of the American Nuclear Society 77, 114–116.
Mi, Y., Ishii, M., Tsoukalas, L.H., 1998. Vertical two-phase flow identification using advanced instrumentation and neural networks. Nuclear Engineering and Design 184, 409–420.
Orion, I., Wilopolski, L., 2002. Limitations in the PHOTON Monte Carlo gamma transport code. Nuclear Instruments and Methods in Physics Research A 480, 729–733.
Pelowitz, D.B., 2005. MCNP-X TM User's Manual, Version 2.5.0. LA-CP-05–0369. Los Alamos National Laboratory.
Saito, K., Moriuchi, S., 1981. Monte Carlo calculation of accurate response functions for a NaI(Tl) detector for gamma rays. Nuclear Instruments and Methods 185, 299–308.
Salgado C.M., Brandão L.E., Schirru, R., Pereira, C.M.N.A., Ramos, R., Silva, A.X., 2007. Study of volume fractions for stratified and annular regime in multiphase flows using gamma-rays and artificial neural network. In: 5th International Nuclear Atlantic Conference – INAC, Santos, SP, BR.
Salgado, C.M., Brandão, L., Schirru, R., Pereira, C.M.N.A., Ramos, R., Silva, A.X., 2008. Modelagem de detector NaI(Tl) usando MCNP-X. n 0189. XI Encontro de Modelagem Computacional, Volta Redonda, RJ.
Salgado, C.M., Brandão, L.E., Pereira, C.M.N.A., Ramos, R., Silva, A.X., Schirru, R., 2009. Prediction of volume fractions in three-phase flows using nuclear technique and artificial neural network. Applied Radiation and Isotopes ARI 4470.
Shi, Hu-Xia, Chen, Bo-Xian, Li, Ti-Zhu, Yun, D.I., 2002. Precise Monte Carlo simulation of gamma-ray response functions for a NaI(Tl) detector. Applied Radiation and Isotopes 57, 517–524.

Sood, A., Gardner, R.P., 2004. A new Monte Carlo assisted approach to detector response functions. Nuclear Instruments and Methods in Physics Research Section B 213, 100–104.
Tjugum, S.A., Johansen, G.A., Holstad, M.B., 2001. The use of gamma radiation in fluid flow measurements. Radiation Physics and Chemistry 61, 797–798.
Tjugum, S.A., Frieling, J., Johansen, G.A., 2002. A compact low energy multibeam gamma-ray densitometer for pipe-flow measurements. Nuclear Instruments and Methods in Physics Research B 197, 301–309.
X-5 Monte Carlo Team, 2003. MCNP – A General Monte Carlo N-Particle Transport Code, Version 5 Volume I: Overview and Theory, LA-UR-03-1987. Los Alamos National Laboratory.